Microscale simulations of extreme events in complex terrain driven by mesoscalar budget components

Matias Avila[1], O. Lehmkuhl[1] , J. Navarro[2] , J.F. González-Rouco[3] , D. Paredes[4] , G. Díaz-Marta[4] and H. Owen[1]

[1] Barcelona Supercomputing Center(BSC), Barcelona, Spain.
[2] División de Energías Renovables, CIEMAT, Madrid, Spain.
[3] Física de la Tierra y Astrofísica dept. IGEO (UCM-CSICC), Madrid, Spain.
[4] Iberdrola Renovables Energía, Madrid, Spain.

E-mail: matias.avila@bsc.es

Abstract. In this work, we apply a downscaling strategy to analyze extreme weather events that may impact wind farm operation. The coupling applies mesoscale momentum budget components (tendencies) from the WRF model as forcing terms to the governing microscale equations. Our study focuses on flow over complex terrain during specific days to reproduce extreme weather events that produced wind turbine damage. The interaction of the meso- and micro-scale features are relevant in the simulation of extreme conditions. The simulation results are compared with observations from nacelle anemometers of the wind turbines in two different wind farms by analyzing time series and wind profiles.

The microscale code Alya, developed at the Barcelona Supercomputing Center (BSC), is closed with URANS and LES closures to solve the momentum and energy equations. Both closures use the same mesoscalar to microscalar coupling methodology and are used in this work to simulate the wind flow. We present the implementation of the mesoscalar coupling to the microscale solver when using URANS and LES closures.

We show that the coupling via tendencies has excellent potential for understanding transient events under extreme weather conditions in very complex terrain. The wind industry can use such simulations to enhance forensic analysis in cases of wind turbine accidents or any other event that may impact turbine operation, such as high turbulence phenomena. We test the ability of the meso- to microscale coupling model to reproduce extreme events with regard to quantities of interest in wind energy.

Simulation results using URANS and LES closures agree reasonably well with observations. In some scenarios, the LES provides results that are closer to measurements. LES models have the advantage of providing wind gusts. We compare the accuracy and performance (CPU-time) of the URANS vs. LES approaches.

1. Introduction

The increasing size of wind turbines, with rotor diameter already spanning more than 150m, requires proper modeling of the atmospheric boundary layer (ABL) from the surface to the free atmosphere. Local processes in the ABL are affected by meso- and large-scale circulations. An efficient way to obtain a high fidelity local-flow structure while incorporating large-scale variability is to couple a microscale and a numerical weather prediction code [1].

In this work, we apply a downscaling strategy to simulate extreme weather events that occurred in the past and had an impact on wind farm operation, affecting a known wind

turbine. The methodology involves solving the mesoscalar flow during the dates of interest, using the Wind Resource and forecasting model (WRF) in Reanalysis mode. The horizontal mesh resolution used in WRF goes from 27km to 3kms using a nesting down strategy. The wind solved with the latest resolution is coupled to the microscalar simulation through mesoscale momentum budget components (tendencies) from the WRF model as forcing terms to the governing microscale equations [1, 2, 3].

Our study focuses on flow over complex terrain, where the current downscaling strategy will be tested. The interaction of the meso- and micro-scale features are relevant in the simulation of extreme conditions. The simulation results are compared with observations from meteorological towers or wind turbine nacelles in two wind farms by analyzing time series and wind profiles.

The microscale code Alya [4], developed at the Barcelona Supercomputing Center (BSC), uses Unsteady Reynolds Averaged Navier Stokes (URANS) and Large Eddy Simulation (LES) closures, both with the same kind of coupling to mesoscale flow. Recently, the Alaiz benchmark [5] presented results of different mesoscale to microscale coupling methodologies in complex terrain. Alya model coupled to WRF obtained a mean normalized BIAS vs. observations of 3.76% and 4.23% using respectively LES and RANS closures. In this work, we present the implementation of the mesoscalar coupling to the microscale solver using URANS and LES closures. We compare the accuracy of the obtained results and the spent CPU time using both closures.

2. Methodology of the modelling strategy

2.1. Mesoscalar modelling

The mesoscalar simulations have been produced using WRF model version V4.1.2 [6], adopting the WRF settings used in the production run of the New European Wind Atlas [7, 8]. Three one-way squared nested domains of (27, 9, 3) km resolution are configured. The first two domains covered the Iberian Peninsula and were run for two days before the downscaling started. The time step was 60 seconds, storing outputs every five minutes. ERA5 reanalysis data were used as both initial and boundary conditions.

2.2. Microscalar modelling

The highly parallelized finite element code Alya [4], developed at Barcelona Supercomputing Center (BSC), is used to solve the microscalar simulations. Alya-URANS and Alya-LES are implementations of URANS and LES turbulence closures in Alya. The URANS model uses the k-ε closure with relevant revisions for ABL flow problems [9] (for implementation details, see [10]). The LES model uses Smagorinsky, Vremann [11] or Deardorff [12] closures. Both closures share implementation using the same linear finite element functions and coupling to mesoscalar flow. Therefore, the obtained differences are due to the turbulence model and mesh size. Alya uses equal spatial interpolation for velocity, pressure, and temperature unknowns. The buoyancy term is modeled using the Boussinesq approximation.

2.2.1. RANS modeling For the URANS model, the momentum, energy, and turbulence equations are solved using a Backward Euler temporal scheme. All the equations are discretized using the Algebraical Subgrid Scale method (ASGS) [13], which gives stability to convection and Coriolis dominating terms in the momentum equation and to convection and reactive terms in the turbulence and energy equations, removing spurious oscillations. The ASGS stabilization method provides pressure stability, allowing equal interpolation spaces for pressure and velocity. The velocity-pressure problem is decoupled using an Orthomin solver [14] that converges to the monolithic scheme.

Once the algebraical system of equations is obtained, a Deflated Conjugate Gradient [15] solver with a linelet pre-conditioner [16] is used to solve the pressure. A Generalized Minimizing

Residual (GMRES) solver is used for the velocity, temperature, and turbulence unknowns.

2.2.2. LES modeling The numerical scheme of the LES model advances in time using an explicit Fractional step method and a third-order Runge Kutta scheme. The spatial discretization of the momentum equation uses a Galerkin scheme, without any stabilization, to minimize the introduced numerical dissipation [17]. The use of a fractional step method [18] introduces a small amount of dissipation enough to avoid stability issues due to the use of equal interpolation spaces for pressure and velocity. The discretization of the convective term in the momentum equation conserves kinetic energy, linear and angular momentum at the discrete level, as it was proposed in [19], providing enhanced results for LES [17]. The energy and the TKE equations are solved explicitly in time using the ASGS method. The convective term in the energy equation is discretized with a skew-symmetric scheme. A Deflated Conjugate Gradient [15] solver with a linelet pre-conditioner [16] is used to solve the pressure.

2.3. Downscaling strategy

Both URANS and LES simulations use the same WRF simulation as mesoscalar input data. The coupling methodology adds horizontally-averaged mesoscale pressure gradient and advection budget terms from WRF to the microscalar momentum equation as volumetric forcing terms. The horizontal averaging is performed at constant height over terrain, obtaining the 1D tendencies approach [1, 2, 3]. While the pressure gradient forces the wind velocity, the advection terms of the mesoscale model account for large-scale variations. We found that the sum of these two mesoscalar budget terms is smoother than just the pressure gradient contribution alone because the advection and pressure gradient terms compensate each other in most situations [3]. Hence, we believe that using the sum of both terms is more appropriate for the coupling.

The microscale energy equation is driven by the mesoscalar surface temperature, which is inferred using Monin- Obukhov similarity theory from the 2 m temperature extracted from WRF. This methodology assumes a uniform potential temperature at ground level, a first approach that could be a source of inaccuracies. We plan to enhance this approach in future work through spatial interpolation of the temperature from WRF at ground level.

WRF writes the budget terms and the 2m potential temperature outputs every 5 min. We found it essential to have a high temporal resolution of WRF outputs in events such as rapid turning of the wind directions. The tendencies are 15 min averaged in time to remove spurious noise.

In all simulations, periodic boundary conditions are imposed laterally, Monin-Obukhov at ground level, and symmetry at the top of the domain.

The microscalar energy equation is coupled to the mesoscalar potential temperature through a nudging term. The nudging coefficient is minimal, being $\tau_{nudg} = 1Day$ [3]. The microscalar temperature inside the ABL is not significantly affected by the nudging term but slowly follows the mesoscalar temperature above the boundary layer height. In the case of extreme events, the mesoscalar temperature may have important variations in time above the ABL, which we found important to follow in the microscale model.

A Rayleigh damping term is applied to the momentum equation of the LES simulation to prevent the reflection of gravity waves off the upper boundary, which could pollute the simulation results. It spans the upper 800m of the computational domain. For URANS simulations, Rayleigh damping was not needed. The effect of including Rayleigh damping in LES runs was subtle. However, we preferred to keep it to prevent any possible pollution of the solution.

The final WRF simulation, which is coupled to microscalar simulation, uses a mesh resolution of 3kms. This resolution is too coarse to capture the orography of the terrain. Thus, only the microscale model accounts for the terrain topography, avoiding double counting effects.

The microscale domains are periodic and have the same extension for URANS and LES simulations.

3. Simulation of wind during extreme weather

We have selected two extreme weather phenomena that impacted wind turbine operation as a test of the developed model chain using WRF and Alya. The coupling technique helps to understand better these events, which are not exclusive to these locations.

3.1. Extreme event on the 1st wind farm

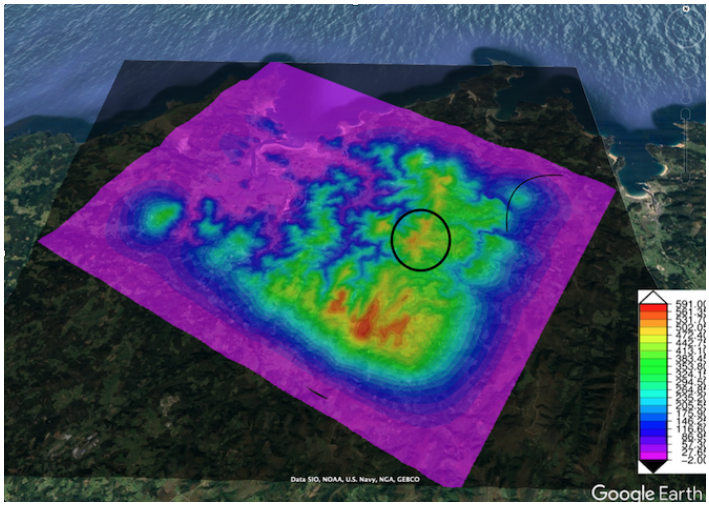

Figure 1. Elevation map of the wind farm, which is circled in black, located at 10 km from the sea coast.

The wind farm described in this section is managed by Iberdrola, located in mountainous terrain just ten kilometers from the sea coast in northern Spain. Fig. 1 shows an elevation map of the computational domain, together with its location on Google Earth. A black circle marks the wind farm region at around 550m above sea level (asl). The wind comes from the West direction, and the computational domain covers the region upwind of the wind farm. The terrain elevation at the periodic boundaries is at sea level to account for the cliffs, which are at the NorthWest of the wind farm.

The computational domain has a horizontal extension of 24km×20km for both LES and URANS simulations. The tangential mesh resolution is 40m at the wind farm, increasing to 300m at the periodic boundaries. The minimum vertical element height is 1.5m for the URANS model and 10m for the LES one. The computational domain is higher than 7kms to allow large wind circulations above the very complex orography. The computational meshes are composed respectively of 5.5 and 8.0 million elements for the LES and URANS simulations.

The wind farm has 22 wind turbines (WTs) with rotor diameter of 47m, and a hub height of 45m; and another two WTs with rotor diameter of 97m, and a hub height of 90. This wind farm has been in operation since 2002. The extreme winds conditions occurred in 2009 between January 22nd and 25th, stirred up by a powerful squall in Great Britain.

The analysis performed here pretends to enhance the understanding around the atmospheric conditions that occurred during the selected days. The analysis focuses particularly on the most affected WT number 25, that remained in stop mode since 5 PM on January 23rd(D1). The wind turbine could not orient its rotor properly when exposed to very high wind speeds. The blades

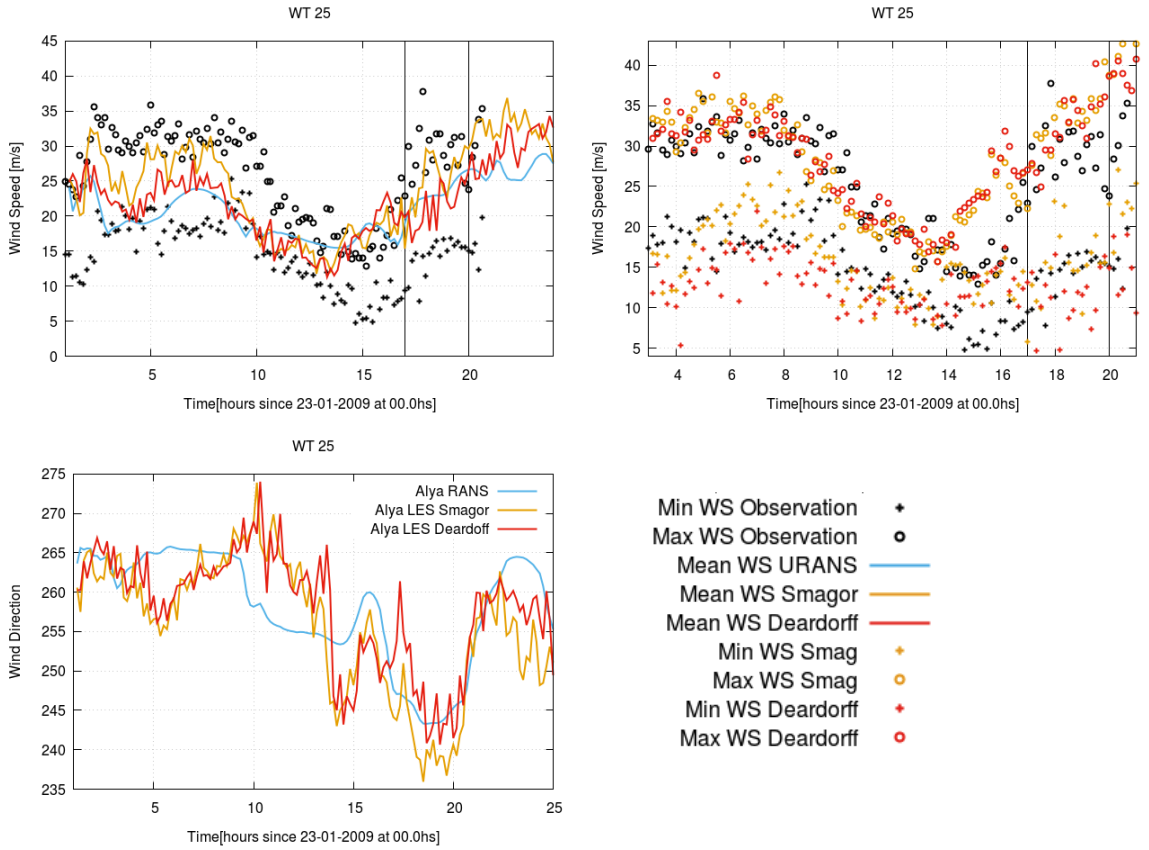

Figure 2. Wind speed (top) and wind direction (bottom left) at the target wind turbine 25 since 23/01/2009 at 00hs (local time). The data points represent the maximum and minimum wind speed measured and LES-modelled every 10 minutes intervals. The filled lines represent 10 min average wind speed values simulated using URANS, Smagorinsky (LES) and Deardorff (LES) models. Bottom Left) 10 min averaged wind direction simulated with URANS, Smagorinsky (LES) and Deardorff (LES) models.

were blocked at a fixed pitch. Therefore, they may have entered into resonance. Communication with all the wind turbines was lost at around 8 PM, suggesting that the damage might have happened shortly before. It is unclear why other turbines were not affected by the extreme weather as much as WT 25.

The mesoscalar simulations started on January 22nd at 0hs, and the coupling with the microscalar model started at 0hs on January 23rd. The initial velocity and temperature conditions in the microscalar simulation are interpolated from WRF. The data measurements provided by Iberdrola at the present wind farm are the maximum and minimum wind speed values measured by the nacelle anemometers in intervals of 10 mins and a sampling rate of 15 s. Unfortunately, the 10 min averaged wind speed, and direction measurements are unavailable. Fig. 2 shows the simulated 10-minute averaged wind speed and wind direction at the target wind turbine 25, together with the maximum and minimum measured wind speeds. There was a communication failure since 8PM (20hs in the figure), so observations are available only for the first 20 hours of simulation. The wind velocity results start being plotted at midnight of January 23rd. The LES results show higher wind speed and direction variations than the URANS model. The Smagorinsky model obtains higher averaged wind speed values than the other models.

The mean wind speed values obtained using the Deardorff LES model are the ones that are most times in the range between the minimum and maximum values of the anemometer measurements. The wind speed obtained with Smagorinsky is typically higher than that obtained using Deardorff, going beyond the maximum measured values. It is observed that, at specific instants, the simulated mean wind speed goes beyond the maximum measured values for all the models. The maximum and minimum wind speeds modeled with LES in intervals of 10 min are also plotted in the figures. Deardorff and Smagorinsky models obtain similar values for maximum wind speed (wind gusts), in fair agreement with observations, except from 14hs to 17hs. However, the Smagorinsky model obtains larger values for the minimum wind speed, reflecting lower TKE values in Fig. 5. The prediction of wind gusts is an advantage of LES modeling over URANS, an output that is relevant for the simulation of this kind of extreme weather events. The obtained wind gusts are not larger than 42 m/s, a value that should not generate damage to the wind turbine. However, such event may be caused by a chain of events of different nature that coincide in time.

The wind turbine event occurs between 17hs and 20hs, marked with two vertical black lines in Fig. 2. During these three hours, wind gusts of more than 35 m/s were measured at the wind turbine nacelle, in agreement with the maximum wind speeds predicted using Deardorff and Smagorinsky models. The averaged wind speed obtained with URANS and Deardorff models has a maximum of 25 m/s. In comparison, the Smagorinsky model obtains averaged velocities up to 30 m/s. Fig. 3 shows modeled and observed wind speed values at WT 26 (adjacent to WT 25) and WT 14. The wind speed values at WT 26 and WT 14 are lower than those at the target WT 25. It is worth noting that the highest simulated wind speed values are obtained between 20hs and 24hs in all WTs (only showed at WT14, 25, and 26).

Fig 4 shows wind velocity and turbulence intensity contour plots at 80m height for the entire wind farm (at 18hs and 20hs of January 23rd), obtained using URANS model. The wind turbines are represented with blue dots, except WT 25 in red. The turbulence intensity (TI) is calculated normalized to a reference wind speed of 15 m/s, being $TI = \frac{\sqrt{2/3\mathrm{TKE}}}{15m/s}$ where TKE refers to the turbulent kinetic energy. The simulated wind speed is not higher at WT 25 than at other WT positions. However, the maximum turbulence intensity, with values larger than 30%, is obtained at WT 25 and upwind.

Fig 5 shows the temporal evolution of the TKE values at different wind turbines. For both LES models, WT 25 is among the turbines with the highest TKE. With the URANS model, the TKE at WT 25 is significantly higher than at any other wind turbine, as observed in Fig4. WT25 is located over a mountain, another mountain exists upstream of WT25, and a valley is found between them. The flow recirculates in the valley generating a wake that reaches WT25, increasing the TKE at its rotor. The k-e method uses a maximum mixing length limitation model that was proposed for the simulation of ABL flows over flat terrain [20], obtaining very accurate solutions. This model is known to produce an artificial lack of diffusion in the wakes generated by the mountainous terrain. Hence, wakes simulated with the present RANS model are generally too long and directional. Unfortunatelly, to the authors knowledge, there is no better way to model ABL flows over complex terrain when using k-ε or k-ω models. The mountainous wakes modeled with LES are more realistic, being broader and more diffuse. Thus, the wake with high TKE reaches a larger number of wind turbines when using LES. While the mixing length limitation is not entirely correct for complex terrain, it highlights that WT 25 has the highest TKE.

We believe that the high TKE values at WT 25 may be the cause that triggered the vibration alarm and stopped the wind turbine. An event such as a turbine damage may be caused by a chain of events of different nature that coincide in time.

It is important to note that Smagorinsky model obtains TKE values that are lower than the obtained using Deardoff and URANS models. The URANS model is calibrated through

parameter $C_\mu = 0.03$ [21] to obtain accurate TKE values over flat and homogeneous terrain. The authors believe that Deardorff model obtains more accurate TKE results than the Smagorinsky model.

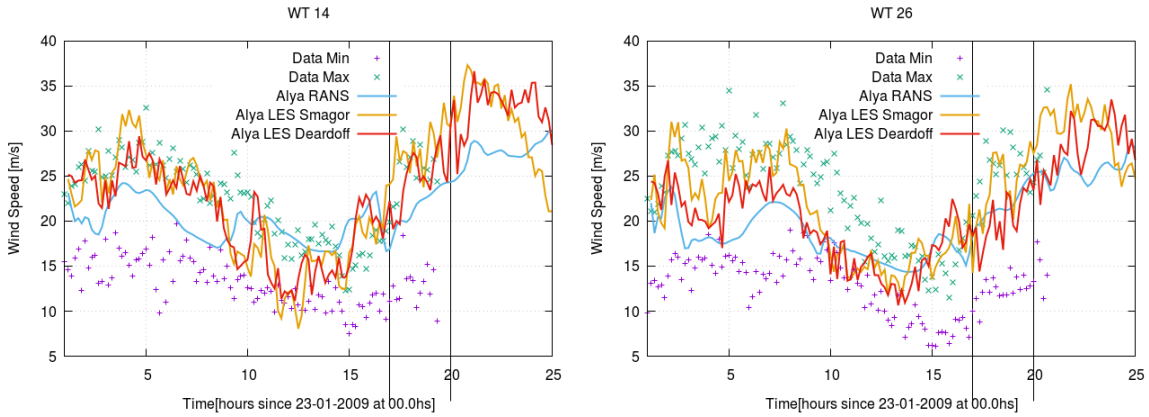

Figure 3. Wind speed at wind turbines 14 and 26 since 23/01/2009 at 00hs (local time). The data points represent the maximum and minimum wind speed measured every 10 minutes intervals, the 10 min averaged wind speed values simulated using URANS, using Smagorinsky (LES) and Deardorff (LES) models.

The LES model used a time step size of 0.35s with a Courant number 3. The URANS model used a time step size of 3.0s. The cpu-time spent by the LES model was around 60% larger than the cpu-time spent by the URANS model.

3.2. Extreme event on the 2nd wind farm

The wind farm described in this section is managed by Iberdrola, located in very mountainous terrain in the Spanish peninsula. This wind farm has been in operation since the year 2000. The wind farm has 30 WTs with a rotor diameter of 47m and a hub height of 45m.. Fig. 6 shows an elevation map of the computational domain, together with its location on Google Earth. The wind farm extends along a ridge, with a maximum height of 1740m asl (WT 18) and a minimum of 1489m asl (WT 1).

The extreme weather event occurred on 19th and 20th March 2018 (D1 and D2, correspondingly). The strong winds at the center of Spain were produced by the Azores anticyclone together with a powerful squall in the North of Scandinavia. Wind Turbine number 17 was strongly affected by the extreme weather on day D2, when abrupt changes of wind direction together with strong gusts occured. The nacelle was wrongly oriented, receiving a tailwind that could cause the bad operating conditions.

The computational domain has the same extension for both URANS and LES simulations, having a tangential mesh resolution of 20m in the zone of the wind turbines for the LES model and 40m for the URANS model. The vertical element height of the elements closer to ground level is 1.5m for the URANS model and 7m when solving with the LES model. The tangential mesh resolution close to the periodic boundaries is 300m. The computational domain is higher than 7kms to allow large wind circulations above the very complex orography. The computational meshes are composed of 7.8 and 6.3 million elements, respectively, for the LES and URANS simulations.

The mesoscalar simulation started on March 18th at 00hs. The coupling with the microscalar simulation started at 10 am on March 19th. The initial velocity and temperature conditions

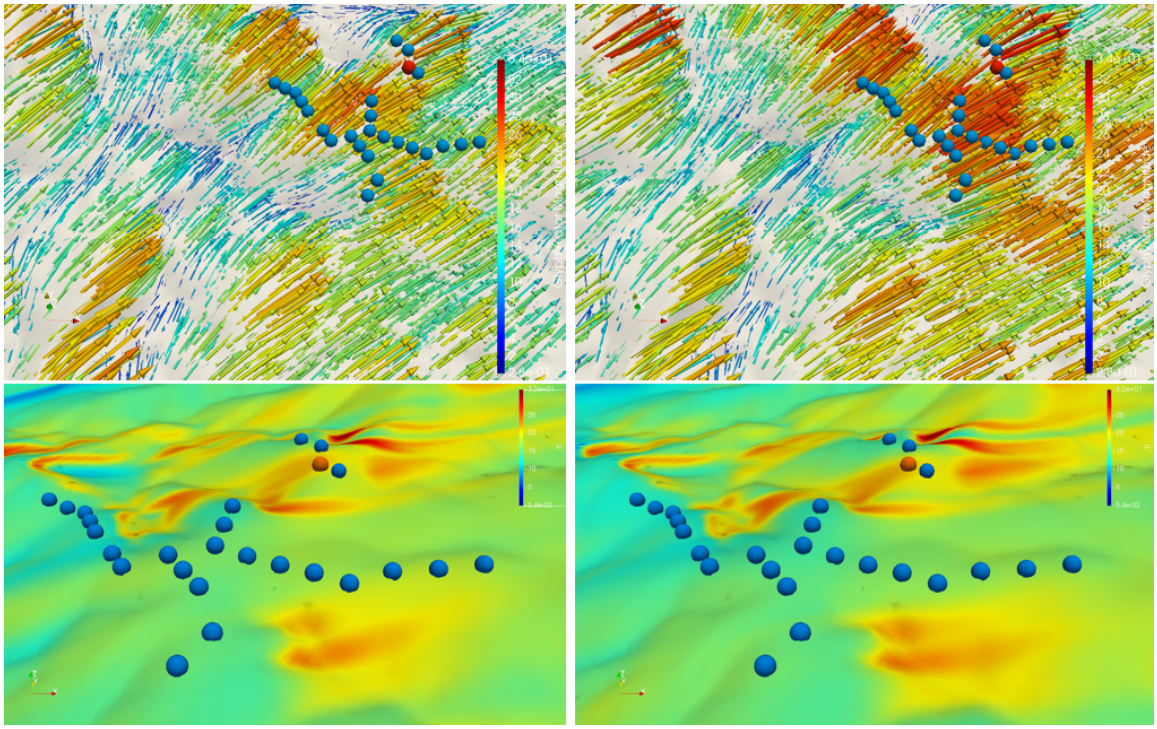

Figure 4. Wind velocity (top) and turbulence intensity (bottom) contour plots at 80m height for all wind turbines (blue dots, except turbine 25 in red) simulated with Alya URANS at 6PM (left) and 8PM (right). Arrows denote wind direction and color wind speed in the velocity plots (top). The maximum values for wind speed are of 34 m/s

in the microscalar simulation are interpolated from WRF solutions. Iberdrola provides 10 min. averaged wind speed values, measured by the nacelle anemometers of each wind turbine. Fig. 7 shows observed and simulated wind speed (10 min averages) at three WTs and simulated wind direction (wind direction measurements are not available) only at the target WT 17. Wind speed measurements increase dramatically during the second day, reaching wind speeds of 50-60 m/s at 10 pm on D2, surpassing design limits. The simulated wind speeds follow the increasing trend for all different runs. However, the URANS model cannot capture the wind speed magnitude measured in either turbine position. The LES model obtains higher wind speeds than the URANS model since 6 am on D2 (30hs in Fig. 7). Hence, the LES models show better agreement against the observed mean wind speed than the URANS model.

Several simulations were run trying to obtain better agreement against observation results at the target WT 17. We included modeling of the forested canopy, interpolating the WRF tendencies at the location of WT17 instead of performing a spatial averaging. The LES were refined to the actual 20m horizontal mesh resolution. However, all simulations obtained similar results, obtaining wind speeds significantly lower than measurements at WT17. A possible reason is that when a wind turbine is not working properly because of a failure, the mesurements at the nacelle may have large errors.

The wind direction obtained from the simulation (Fig. 7) provides valuable information about the event. There is a dramatic wind shift of 130 degrees at 15hs on D1 (from 220º to 350º). The alarm of WT 17 at 16hs showed several emergency flags. After this dramatic wind shift it is possible that WT 17 could not align its rotor with the wind direction.

Fig. 8 shows the wind velocity just before and after the wind shift at 15hs of D1. The shift

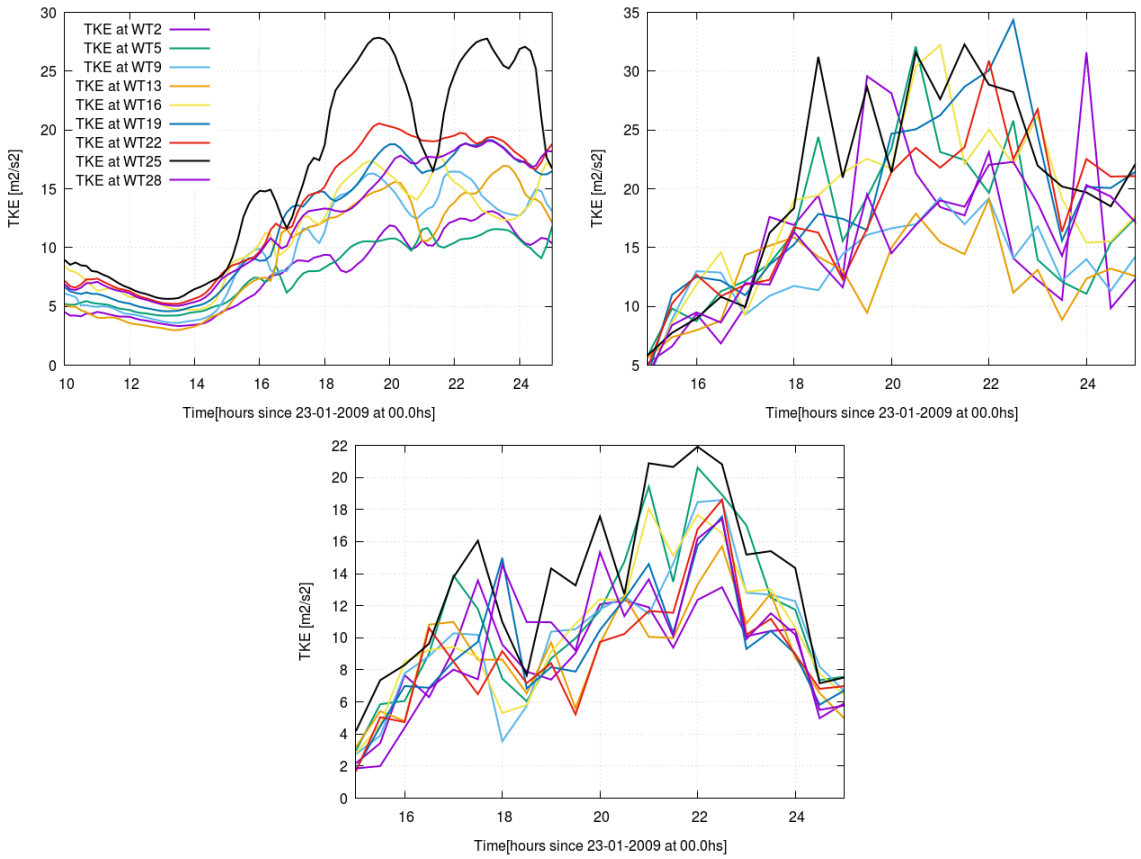

Figure 5. TKE values at different WTs using URANS(top left), LES-Deardorff(top right) and LES-Smagorinsky(bottom)

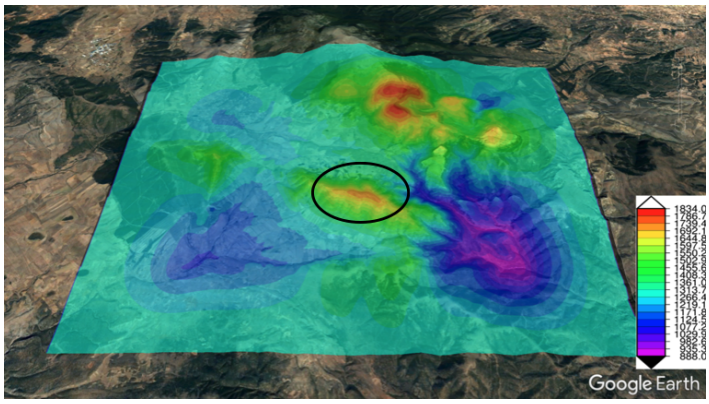

Figure 6. Elevation map of the 2nd wind farm, located in the ridge inside the black circle

occurs at all wind turbine positions. The modeled wind speed has a magnitude of around 15 m/s close to WT17, but the measured wind speed is 20 m/s (Fig. 7) .

Fig. 9 shows contour plots of turbulence intensity, which does not supply additional evidence of specific conditions for WT 17. However, a high TI leeward area extending in the vicinity of

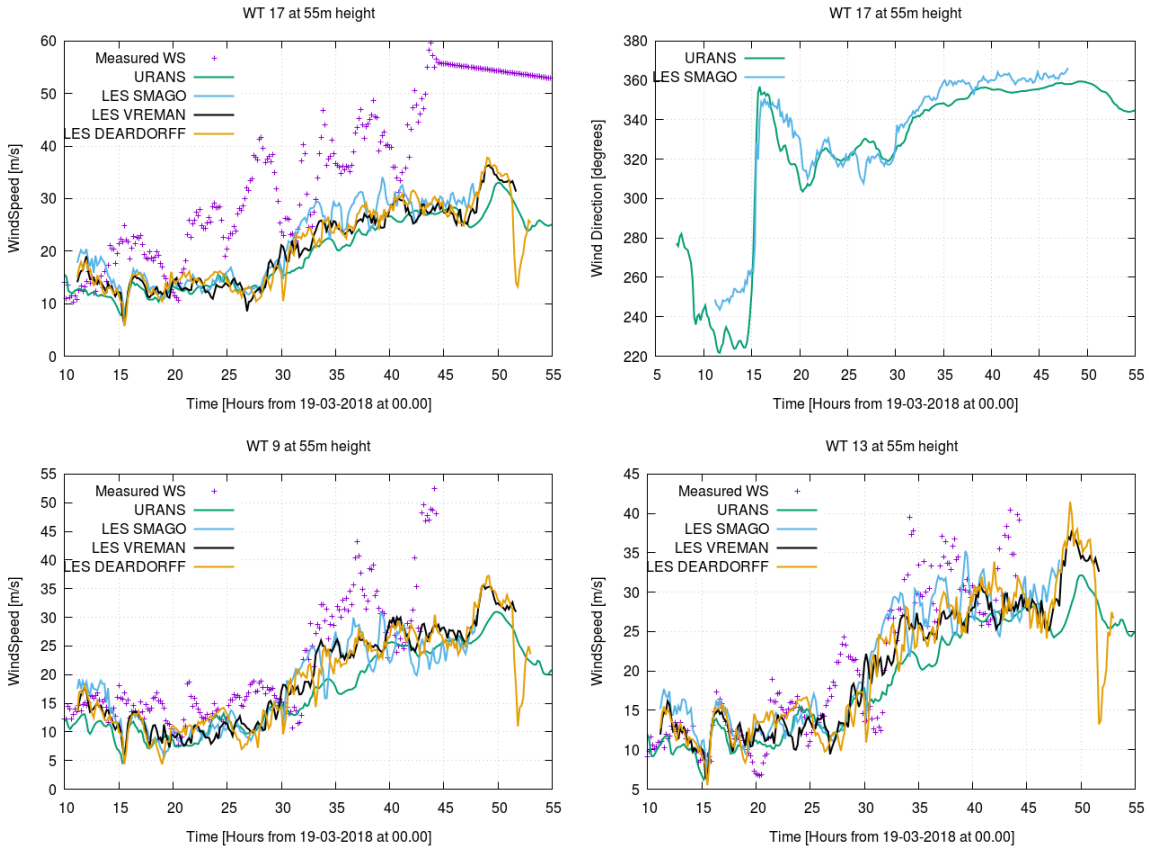

Figure 7. Ten min. averaged wind speed (simulated and measured) and simulated wind direction (top right) at the target wind turbine 17. 10 min. averaged wind speed at other two wind turbines (bottom) since 19/03/2018 at 10am (local time).

WT 17 is observed. It achieves TKE values higher than 50 m2/s2, likely implying intense gusts in the surroundings.

The LES model used a time step size of 0.25s with a Courant number 3. The URANS model used a time step size of 2.5s. The cpu-time spent by the LES models was around 100% larger than the cpu-time spent by the URANS model.

4. Conclusions

While microscale simulations driven by mesoscale tendencies are still a relatively new approach, we showed their potential for better understanding transient events under extreme weather conditions. The wind industry can use such simulations to enhance forensic analysis in cases of accidents, providing better insight to turbine inflow conditions.

This kind of simulation can also be helpful to understand better the flow over complex terrain during wind farm planning. They allow identifying riskier areas within the wind farm in terms of extreme wind speed, gusts, turbulence intensity, or recirculation; helping select wind turbine positions to avoid potential damage under extreme weather conditions.

Simulation results using URANS and LES closures agree reasonably well with observations. However, we observe that the dynamics of the LES simulation results agree a bit better with measurements at the two wind farms analyzed in this work. We believe that the LES closures

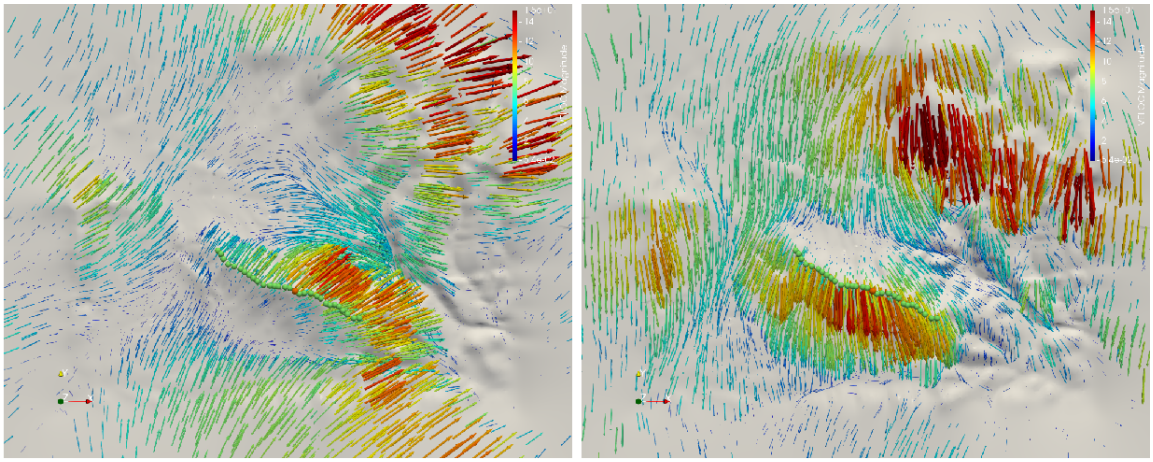

Figure 8. Simulated wind velocity using URANS model just before and after the wind shift on D1: 2:30PM (left) and 3:40PM (right) on D1. Turbine locations are depicted with green dots except for the target wind turbine 17, in red.

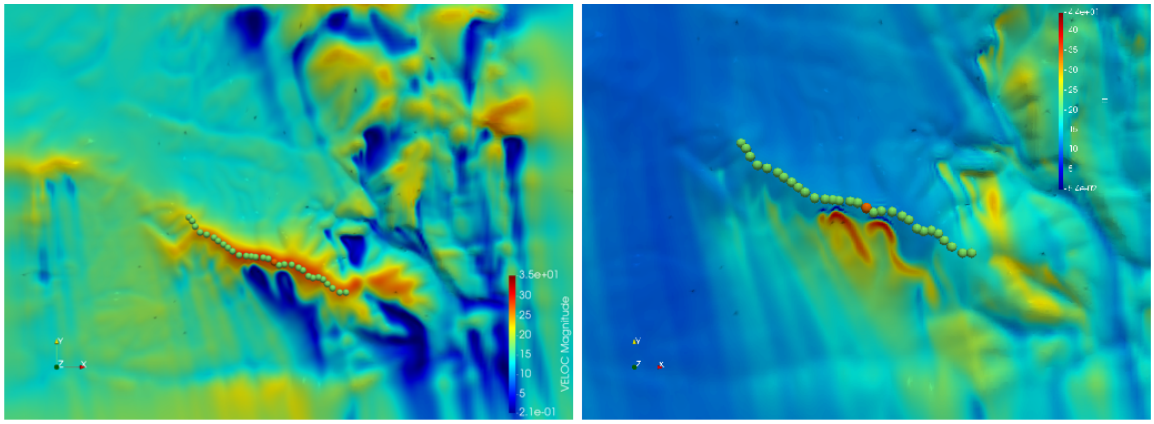

Figure 9. Wind Speed (left) and turbulence intensity (right) contour plots at 80m height. simulated with URANS model at 10PM of D2. Turbines are depicted as green dots and turbine 17 in red color.

model the mountainous wakes better than URANS, because the latter use a maximum mixing length limitation model. This correction needs to be introduced to k-ϵ and k-ω models for proper modeling of Coriolis forces in ABL flows. An advantage of LES model is that is able to model wind gusts with reasonable accuracy.

The LES model spent a cpu-time around 70% to 100% larger than the URANS models. Thus, LES models are not too expensive when compared to URANS models, being a valuable choice for this kind of transient ABL simulations.

A future work that may enhance the simulation results is to consider the spatial dependence of the potential temperature obtained with WRF at ground level in the downscaling strategy.

Acknowledgements
The research leading to these results has been supported by the Supercomputing and Energy for Mexico Project (ENERXICO, European Union's Horizon 2020 Programme, grant agreement

n 828947; and Mexican Department of Energy, CONACYT-SENER Hidrocarburos grant agreement n B-S-69926).

Herbert Owen was supported by the Energy oriented Centre of Excellence II (EoCoE-II), grant agreement number 824158, funded within the Horizon2020 framework of the European Union.

Oriol Lehmkuhl is partially financed by a Ramón y Cajal postdoctoral contract by the Ministerio de Economa y Competitividad, Secretaría de Estado de Investigación, Desarrollo e Innovación, Spain (RYC2018-025949-I).

References

[1] Sanz Rodrigo J, Churchfield M J, Kosović B and Kosovic B 2017 *Wind Energy Science* **2** 35–54 ISSN 2366-7451 URL https://www.wind-energ-sci.net/2/35/2017/
[2] Draxl C, Allaerts D, Quon E and Churchfield M 2021 *Boundary-Layer Meteorology* **179** 73–98 ISSN 15731472 URL https://doi.org/10.1007/s10546-020-00584-z
[3] Olsen B 2018 *Mesoscale to microscale coupling for determining site conditions in complex terrain* Ph.D. thesis Denmark
[4] Vazquez M 2016 *Journal of Computational Science* **14** 15 – 27 the Route to Exascale: Novel Mathematical Methods, Scalable Algorithms and Computational Science Skills
[5] Rodrigo J S, Santos P, Arroyo R C, Avila M, Cavar D, Lehmkuhl O, Owen H, Li R and Tromeur E 2021 *Journal of Physics: Conference Series* **1934** ISSN 17426596
[6] Skamarock C, Klemp B, Dudhia J, Gill O, Liu Z, Berner J, Wang W, Powers G, Duda G, Barker D M and Huang X 2019 A description of the advanced research wrf model version 4
[7] Hahmann A N, Sle T, Witha B, Davis N N, Dörenkämper M, Ezber Y, García-Bustamante E, González-Rouco J F, Navarro J, Olsen B T and Söderberg S 2020 *Geoscientific Model Development* **13** 5053–5078 URL https://gmd.copernicus.org/articles/13/5053/2020/
[8] Dörenkämper M, Olsen B T, Witha B, Hahmann A N, Davis N N, Barcons J, Ezber Y, García-Bustamante E, González-Rouco J F, Navarro J, Sastre-Marugán M, Sle T, Trei W, Žagar M, Badger J, Gottschall J, Sanz Rodrigo J and Mann J 2020 *Geoscientific Model Development* **13** 5079–5102 URL https://gmd.copernicus.org/articles/13/5079/2020/
[9] Sogachev A, Kelly M and Leclerc M 2012 *Boundary-Layer Meteorology* **145** 307–327 ISSN 0006-8314
[10] Barcons J, Avila M and Folch A 2019 *Wind Energy* **22** 269–282 URL https://onlinelibrary.wiley.com/doi/abs/10.1002/we.2283
[11] Vreman A W 2004 *Physics of Fluids* **16** 3670–3681
[12] Deardorff J W 1980 *Boundary-Layer Meteorology* **18** 495–527
[13] Codina R 1998 *Computer Methods in Applied Mechanics and Engineering* **156** 185 – 210 ISSN 0045-7825
[14] Houzeaux G, Aubry R and Vazquez M 2011 *Computers & Fluids* **44** 297 – 313 ISSN 0045-7930
[15] Lohner R, Mut F, Cebral J R, Aubry R and Houzeaux G 2011 *International Journal for Numerical Methods in Engineering* **87** 2–14 ISSN 1097-0207
[16] Soto O, Lohner R and Camelli F 2003 *International Journal of Numerical Methods for Heat & Fluid Flow* **13** 133–147
[17] Lehmkuhl O, Houzeaux G, Owen H, Chrysokentis G and Rodriguez I 2019 *Journal of Computational Physics* **390** 51–65 ISSN 0021-9991 URL https://www.sciencedirect.com/science/article/pii/S0021999119302372
[18] Codina R 2001 *Journal of Computational Physics* **170** 112–140 ISSN 00219991
[19] Charnyi S, Heister T, Olshanskii M A and Rebholz L G 2017 *Journal of Computational Physics* **337** 289–308 ISSN 0021-9991
[20] Apsley D and Castro I 1997 *Boundary-Layer Meteorology* **83** 75–98
[21] Ivanell S, Arnqvist J, Avila M, Cavar D, Chavez-arroyo R A, Olivares-espinosa H, Peralta C, Adib J and Witha B 2018 *Wind Energy Science Discussions* **20**